Gα12 regulates protein interactions within the MDCK cell tight junction and inhibits tight-junction assembly

Ernesto Sabath[1,*], Hideyuki Negoro[1,*], Sarah Beaudry[1], Manuel Paniagua[1], Susanne Angelow[2], Jagesh Shah[1], Nicholas Grammatikakis[3], Alan S. L. Yu[2] and Bradley M. Denker[1,‡]

[1]Renal Division, Brigham and Women's Hospital and Harvard Medical School, Boston, MA 02115, USA
[2]Nephrology Division, University of Southern California, Los Angeles, CA 90089, USA
[3]Institute of Biology, National Centre for Scientific Research 'Demokritos', Athens, Greece

*These authors contributed equally to this work
‡Author for correspondence (e-mail: bdenker@rics.bwh.harvard.edu)

Accepted 11 December 2007
Journal of Cell Science 121, 814-824 Published by The Company of Biologists 2008
doi:10.1242/jcs.014878

Summary

The polarized functions of epithelia require an intact tight junction (TJ) to restrict paracellular movement and to separate membrane proteins into specific domains. TJs contain scaffolding, integral membrane and signaling proteins, but the mechanisms that regulate TJs and their assembly are not well defined. Gα12 (GNA12) binds the TJ protein ZO-1 (TJP1), and Gα12 activates Src to increase paracellular permeability via unknown mechanisms. Herein, we identify Src as a component of the TJ and find that recruitment of Hsp90 to activated Gα12 is necessary for signaling. TJ integrity is disrupted by Gα12-stimulated Src phosphorylation of ZO-1 and ZO-2 (TJP2); this phosphorylation leads to dissociation of occludin and claudin 1 from the ZO-1 protein complex. Inhibiting Hsp90 with geldanamycin blocks Gα12-stimulated Src activation and phosphorylation, but does not affect protein levels or the Gα12–ZO-1 interaction. Using the calcium-switch model of TJ assembly and GST-TPR (GST-fused TPR domain of PP5) pull-downs of activated Gα12, we demonstrate that switching to normal calcium medium activates endogenous Gα12 during TJ assembly. Thrombin increases permeability and delays TJ assembly by activating Gα12, but not Gα13, signaling pathways. These findings reveal an important role for Gα12, Src and Hsp90 in regulating the TJ in established epithelia and during TJ assembly.

Supplementary material available online at
http://jcs.biologists.org/cgi/content/full/121/6/814/DC1

Key words: Epithelial cells, G proteins, G12, Kidney, Tight junctions

Introduction

The epithelial cell tight junction (TJ) is the most apical component of the junctional complex. The TJ defines the polarized epithelial phenotype by establishing the barrier to paracellular molecular movement and by providing the fence, restricting the localization of proteins into the apical or basolateral domains. Disruption and reassembly of TJs is an important component of epithelial injury and repair, and contributes to the development of several kidney diseases (Lee et al., 2006). Numerous proteins are found within the TJ, including the transmembrane proteins occludin and junctional adhesion molecule (JAM). However, the claudin family of transmembrane proteins is responsible for the barrier function (Furuse et al., 1998). In addition, the TJ also contains numerous scaffolding proteins, including the zona-occludens family members ZO-1, ZO-2 and ZO-3 (TJP1, TJP2 and TJP3, respectively), as well as signaling proteins and other unique TJ proteins. There are numerous interactions among TJ proteins, and many of the proteins are linked to the actin cytoskeleton (reviewed in Matter and Balda, 2003). The specific claudins expressed in epithelia are the major determinant of the paracellular properties (Tsukita et al., 2001). The barrier function is also regulated in response to physiological stimuli (reviewed in Nusrat et al., 2000). The finding of numerous signaling proteins within the TJ and the importance of phosphorylation is consistent with extracellular signal regulation of the barrier (see Denker and Nigam, 1998; D'Souza et al., 2005). Furthermore, the biogenesis of the TJ in developing epithelial tissues or after injury involves numerous signaling pathways, which include PKC, Src, small G proteins (Rho and Rac) and G proteins (Gαi2, Gαs) (reviewed in Matter and Balda, 2003).

Heterotrimeric G proteins regulate fundamental cellular properties through their Gα and Gβγ subunits (reviewed in Neer, 1995). In addition to signaling from plasma membrane receptors, Gα subunits are also localized in numerous intracellular compartments and have been implicated in other cellular functions, including vesicular trafficking (Pimplikar and Simons, 1993), protein processing through the Golgi (Stow et al., 1991) and cytokinesis (Blumer et al., 2002). The Gα12/13 family regulates stress-fiber formation and other crucial cellular functions via numerous pathways. Several groups have described Gα subunits (including Gα12; GNA12) localized to the epithelial cell TJ (de Almeida et al., 1994; Dodane and Kachar, 1996; Ercolani et al., 1990; Hamilton and Nathanson, 1997) and implicated G proteins in regulation of barrier function and TJ assembly (Balda et al., 1991). In the calcium-switch model of TJ assembly (Cereijido et al., 1993; Rodriguez-Boulan and Nelson, 1989), we demonstrated that Gαo, Gαi2 and Gαs stimulate TJ assembly, but only Gαi2 affected baseline TJ properties (Denker et al., 1996; Saha et al., 1998; Saha et al., 2001). We have previously shown that Gα12 and ZO-1 directly interact, and activation of Gα12 leads to TJ disruption and increased permeability (Meyer et al., 2002). The ZO-1-binding site for Gα12 was identified and, upon Gα12 activation, Src but not Rho is activated, leading to disruption of the TJ (Meyer et al., 2003; Meyer et al., 2002). However, the mechanisms regulating the TJ via Gα12 are not known and a potential role for Gα12 in regulating

TJ assembly has not been investigated. Herein, it is shown that Gα12 activates Src via a mechanism that uses the heat shock protein (Hsp)90 chaperone. Hsp90 interacts with activated [thrombin-stimulated or constitutively active QL (glutamine to lysine substitution)] Gα12, but not to inactive Gα12. Src phosphorylates ZO-1 and ZO-2, resulting in loss of claudin 1 and occludin interactions with ZO-1, and inhibition of Hsp90 with geldanamycin blocks these events and prevents barrier disruption. Furthermore, we show for the first time that endogenous Gα12 is activated during TJ assembly in the absence of receptor agonists, and that thrombin stimulation of endogenous Gα12, but not Gα13, increases permeability in intact monolayers and delays TJ assembly.

Results

Gα12 expression in MDCK cells does not affect levels of TJ proteins

Tet-off-inducible wild-type Gα12 and QLα12 (constitutively active mutant, Q229L) were expressed in Madin-Darby canine kidney (MDCK) cells and have been previously characterized (Meyer et al., 2003; Meyer et al., 2002). Supplementary material Fig. S1 shows the inducible expression of wild-type Gα12 and QLα12 in MDCK cells with the removal of doxycycline (–dox) for 72 hours; there were no differences in the expression levels of TJ proteins.

Src is a component of the TJ complex and regulates permeability

We previously demonstrated Src-dependent changes in permeability and TJ structure in QLα12-MDCK cells (Meyer et al., 2003). To further characterize the Gα12-stimulated loss of barrier function, Gα12- and QLα12-MDCK cells [with/without (+/–) dox] were analyzed for transepithelial resistance (TER, a measure of monolayer ionic permeability), and Na^+ and Cl^- permeability. Supplementary material Fig. S2A confirms a small reduction in TER in Gα12-MDCK cells and a significant reduction in QLα12-MDCK cells. The QLα12-stimulated reduction in TER is nearly completely inhibited with the Src-specific inhibitor PP2. Consistent with TER data, inhibition of Src with PP2 completely blocked the permeability changes induced with QLα12 expression (supplementary material Fig. S2B,C, and discussed in more detail later).

To determine whether Src is part of the TJ complex, ZO-1 was immunoprecipitated from Gα12-MDCK cells and probed by western blotting for Src. Fig. 1A shows that Src immunoprecipitates with ZO-1 in QLα12-MDCK cells independently of Gα12 expression (+/–dox). Controls with rat ascites or beads alone failed to precipitate Src. A similar experiment was repeated in Gα12- and QLα12-MDCK cells (+/–dox), and the ZO-1 immunoprecipitates were probed by western blotting for active Src (anti-pTyr419) and ZO-1 (Fig. 1B). The amount of inactive Src that co-precipitated with ZO-1 was similar in the four conditions (not shown), but in both Gα12- and QLα12-MDCK cells there was increased pTyr419 detected in the ZO-1 precipitates of –dox cells. This is consistent with activated Src interacting with the ZO-1 protein complex in both Gα12- and QLα12-expressing MDCK cells. To determine colocalization of ZO-1 and Src in MDCK cells, Gα12-MDCK cells (+/–dox) were analyzed by confocal microscopy. Fig. 1C, panels a (+dox) and h (–dox) show a merged image of ZO-1 and Src. To determine the extent of overlap for these proteins, a single cell was identified (Fig. 1C, white box in panels a,h). ZO-1 (Fig. 1C, green), Src (Fig. 1C, red) and merged images are shown at high magnification in the *x-y* orientation [Fig. 1Cb-d (+dox) and i-k (–dox)]. Next, one membrane region was highlighted (Fig. 1C, white enclosed region) and examined in the *x-z* orientation [Fig. 1C, lat-z, panels e-g (+dox) and l-n (–dox)]. In the absence of Gα12 expression (+dox), ZO-1 was found in a discrete apical region (Fig. 1Ce) and Src was detected in a broader domain of the lateral membrane (Fig. 1Cf) with some overlap in the apical domain (Fig. 1Cg). With Gα12 expression (–dox), ZO-1 was more widely distributed within the lateral membrane (Fig. 1Cl-n). This suggests that activation of Src with Gα12 expression (see also Fig. 1B, Fig. 2D and Fig. 3C) is sufficient to induce subtle changes in ZO-1 localization. Taken together with the co-immunoprecipitation of Src with ZO-1, these results reveal that a fraction of Src colocalizes with ZO-1 in both conditions (+/– dox).

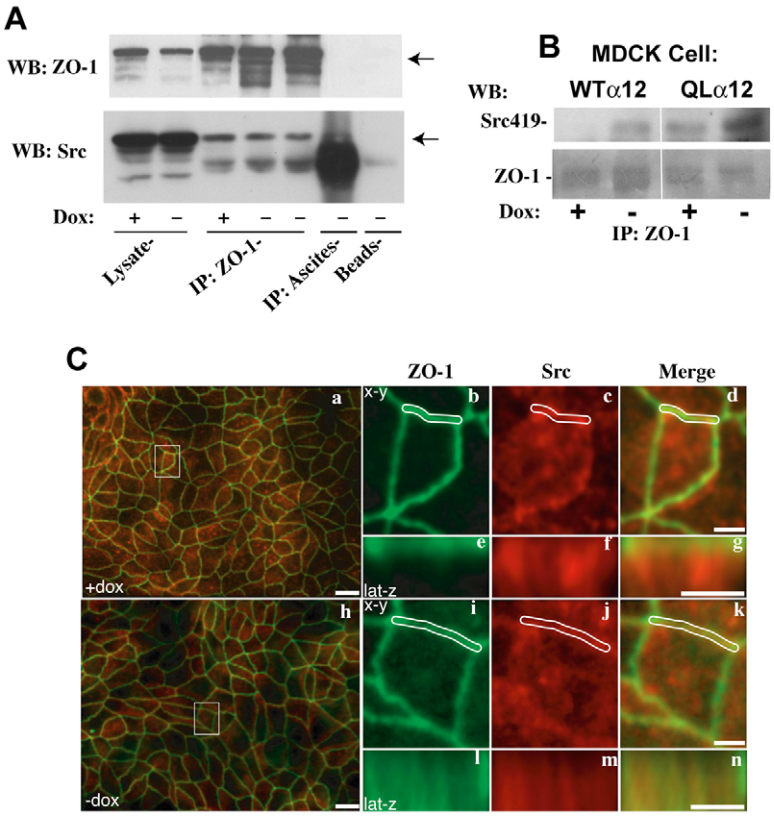

Fig. 1. Src is a component of the TJ complex. (A) Western blots for ZO-1 and total Src after ZO-1 immunoprecipitation from QLα12-MDCK cells in +/–dox conditions. ZO-1 hybridoma was added undiluted to an equivalent amount of cell lysates prepared as described in the Materials and Methods. Negative controls were rat ascites using IgG beads. Arrows indicate the ZO-1 and Src bands. (B) Lysates from Gα12- and QLα12-MDCK cells (+/–dox) were immunoprecipitated with ZO-1 and probed with antibodies against active Src (pTyr419) and ZO-1. (C) Confocal microscopy of Gα12-MDCK cells +/–dox double stained for ZO-1 and Src as described in the Materials and Methods. (Ca,Ch) White box indicates the cell that was examined at higher magnification in the panels to the right. In *x-y* and lat-z panels, a region of the membrane was identified (white enclosure) for additional analysis. The lat-z images represent the apical 5 μm region of the cell (total height approximately 8 μm). (Ca-Cg) +dox; (Ch-Cn) –dox. FITC-ZO-1, Texas-red c-Src and merged images are shown for both conditions in *x-y* and lat-z orientation. Scale bars: 10 μm (Ca,Ch), 5 μm (Cb-Cg,Ci-Cn).

QLα12 stimulates Src tyrosine phosphorylation of ZO-1 and ZO-2

To characterize the tyrosine phosphorylation of TJ proteins, QLα12-MDCK cells (+/–dox) were cultured with or without PP2 (Src inhibitor) or genistein (inhibits numerous tyrosine kinases). Immunoprecipitations of ZO-1, ZO-2, occludin (Fig. 2), claudin 1 and claudin 2 (not shown) were followed by phosphotyrosine western blots. In Fig. 2, the first panel shows tyrosine phosphorylation of ZO-1 (Fig. 2A), ZO-2 (Fig. 2B) and occludin (Fig. 2C) in +/–dox conditions. With induction of QLα12, the tyrosine phosphorylation of ZO-1 (Fig. 2A) and ZO-2 (Fig. 2B) was significantly increased (two- to three-fold), whereas there was no significant change for occludin (Fig. 2C). No tyrosine phosphorylation of claudin 1 and claudin 2 was detected under any condition (not shown). In Gα12-MDCK cells there was significantly less tyrosine phosphorylation of ZO-1 at baseline (+dox), although a small increase was seen with Gα12 expression (–dox; Fig. 2D). It was difficult to detect any baseline or stimulated tyrosine phosphorylation of ZO-2 or occludin in Gα12-MDCK cells (not shown). Pre-treatment of QLα12-MDCK cells with either PP2 or genistein inhibited QLα12-stimulated ZO-1 phosphorylation to levels that were similar to the +dox control. The stimulation of ZO-2 tyrosine phosphorylation with QLα12 expression was threefold higher than in controls and, unlike ZO-1, was completely inhibited with PP2 and genistein to levels significantly below basal. Tyrosine phosphorylation on occludin was not significantly affected by the tyrosine kinase inhibitors.

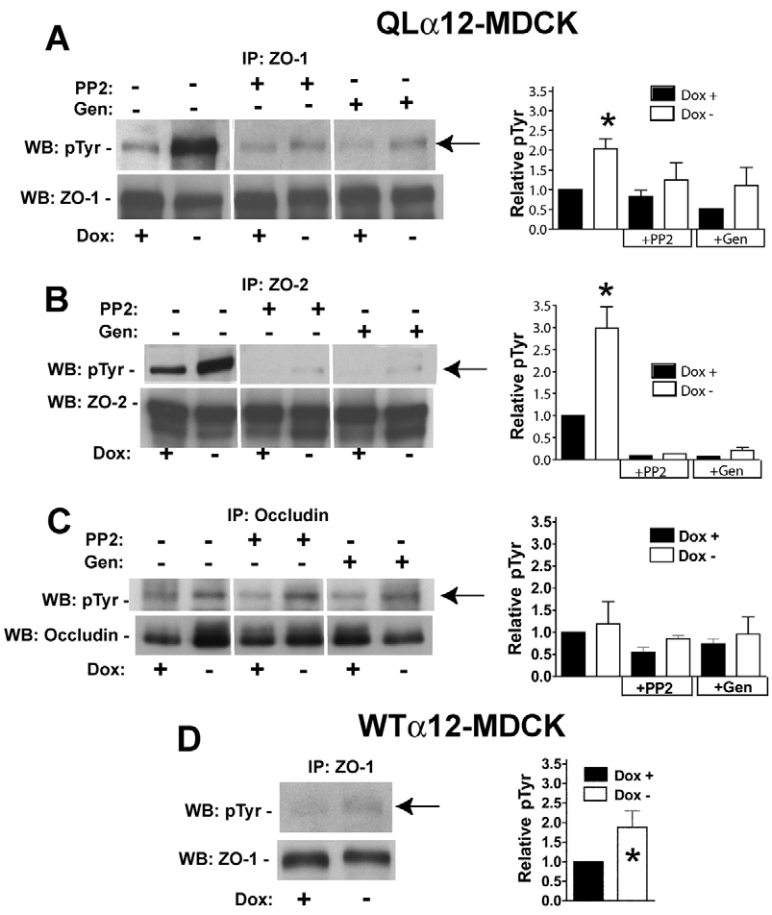

Fig. 2. ZO-1 and ZO-2 are tyrosine phosphorylated in QLα12-MDCK cells by Src. Immunoprecipitations of the indicated TJ proteins were performed as described in the Materials and Methods followed by western blotting with 4G10 antibody. Identical amounts of lysate from QLα12-MDCK cells +/–dox for 72 hours were used for each precipitation. Immunoprecipitations were repeated from cells cultured in PP2 (10 μM) or genistein (2 μM), which were added to the medium at the time of medium change to –dox. The intensity of the phosphotyrosine (pTyr) band (arrows) in each condition is normalized to the amount of protein in the precipitate. This fraction was divided by the fraction of pTyr detected in +dox cells with no inhibitor condition. Bar graphs on the right summarize the results from three experiments. (A) ZO-1; (B) ZO-2; (C) occludin; and (D) ZO-1 in Gα12-MDCK +/–dox. *P<0.05.

QLα12 disrupts occludin and claudin 1 interactions with ZO-1

The epithelial cell TJ in MDCK cells contains a complex of interacting proteins (reviewed in Matter and Balda, 2003). We next asked whether Gα12-Src-stimulated tyrosine phosphorylation of ZO-1 and ZO-2 affected protein-protein interactions within the TJ. ZO-1 was immunoprecipitated and interacting proteins analyzed by western blot. Fig. 3A shows that control immunoprecipitations with rat ascites did not precipitate ZO-1 from QLα12-MDCK cells +/–dox, whereas 2-4% of total ZO-1 was immunoprecipitated with ZO-1 hybridoma under these conditions. Gα12 expression in MDCK cells (+/–dox) did not affect the amount of immunoprecipitated ZO-1 (Fig. 3B) and reprobing the blot with antibodies to other TJ proteins demonstrated that the interaction between ZO-2 or occludin with the ZO-1 complex was not affected. However, there was a small but consistent reduction in the amount of claudin 1 interacting with the ZO-1 complex (24±7%; n=3) (Fig. 3B,C). Like in Gα12-MDCK cells, in QLα12-MDCK cells there were no changes in the amount of ZO-1 precipitated nor of co-precipitated ZO-2 (Fig. 3B). However, there was significant loss of occludin and nearly complete disruption of claudin 1 (Fig. 3B,C; 54±12% and 75±15%, respectively) from the ZO-1 complex. To determine whether Src modulated these protein interactions, the immunoprecipitations were repeated in cells treated with PP2. As shown in Fig. 3B,C, Src inhibition completely prevented the loss of occludin and claudin 1 from the ZO-1 complex. These findings suggest that Gα12/Src-stimulated tyrosine phosphorylation of ZO-1 and ZO-2 leads to disruption of TJ-protein interactions.

The dissociation of claudin 1 from the ZO-1 complex was further characterized by double labeling and immunofluorescence microscopy. Supplementary material Fig. S3A confirms the previously reported localization of ZO-1 and claudin 1 in +/–dox and in –dox +PP2 QLα12-MDCK cells (Meyer et al., 2003). In +dox conditions, both ZO-1 and claudin 1 were localized along the basolateral membrane with partial overlap. With QLα12 expression (–dox) there was a loss of barrier function (supplementary material Fig. S2), and disruption of ZO-1 and claudin 1 staining (supplementary material Fig. S3A). Pre-treatment of QLα12-MDCK cells with the Src inhibitor PP2 blocked the changes in ZO-1 and claudin 1 staining patterns (supplementary material Fig. S3A). Finally, the redistribution of claudin 1 was examined biochemically with detergent extraction (supplementary material Fig. S3B). Claudin 1 was approximately 51±5% (n=2) soluble in +dox conditions, but became more resistant to detergent extraction with QLα12 expression (26±7% soluble in –dox conditions). Consistent with the immunoprecipitation and immunofluorescence microscopy

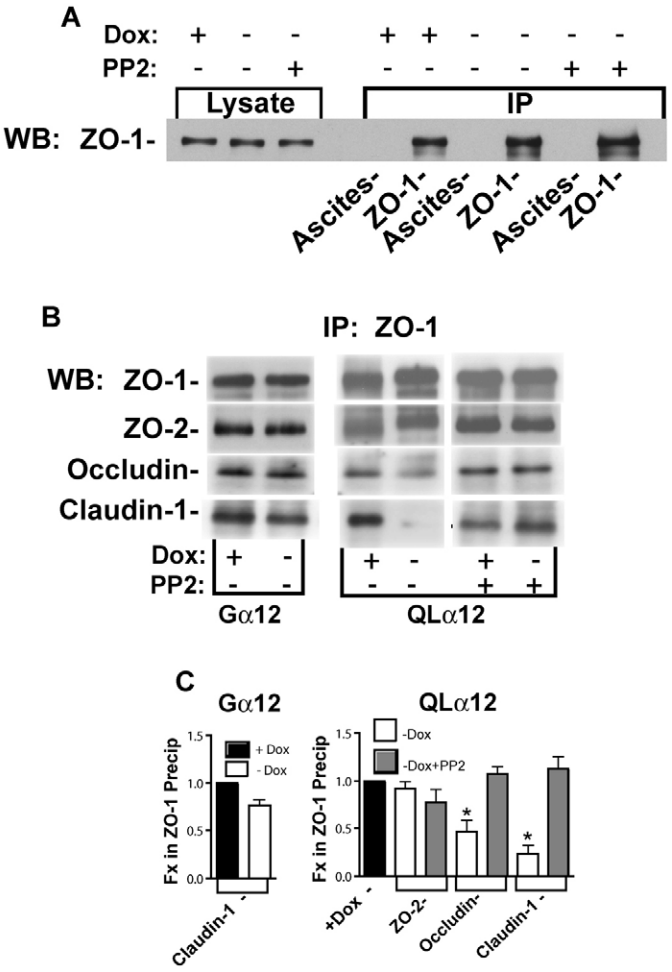

Fig. 3. Gα12/Src activation disrupts interactions of claudin 1 and occludin with ZO-1. (A) Specificity of ZO-1 immunoprecipitations. Gα12-MDCK cells were cultured +/–dox +/–PP2 and immunoprecipitated with rat monoclonal R46 antibody or the equivalent amount of ascites control. Western blot for ZO-1 in cell lysates and immunoprecipitations using the identical antibody is shown. (B) Gα12- and QLα-12 MDCK cells +/–dox were immunoprecipitated with ZO-1 antibody as described in the Materials and Methods. Immunoprecipitates were analyzed by western blotting to ZO-1 followed by reprobing with antibodies to other TJ proteins (ZO-2, occludin and claudin 1). A parallel analysis was performed in QLα12-MDCK cells pre-treated with the Src inhibitor PP2 (10 μM) added at the time of switch to –dox medium. (C) Bar graphs summarizing the fraction of TJ protein remaining associated with ZO-1. The results are the mean ± s.e.m. of three experiments normalized to the ZO-1 immunoprecipitates (+dox). *P<0.05.

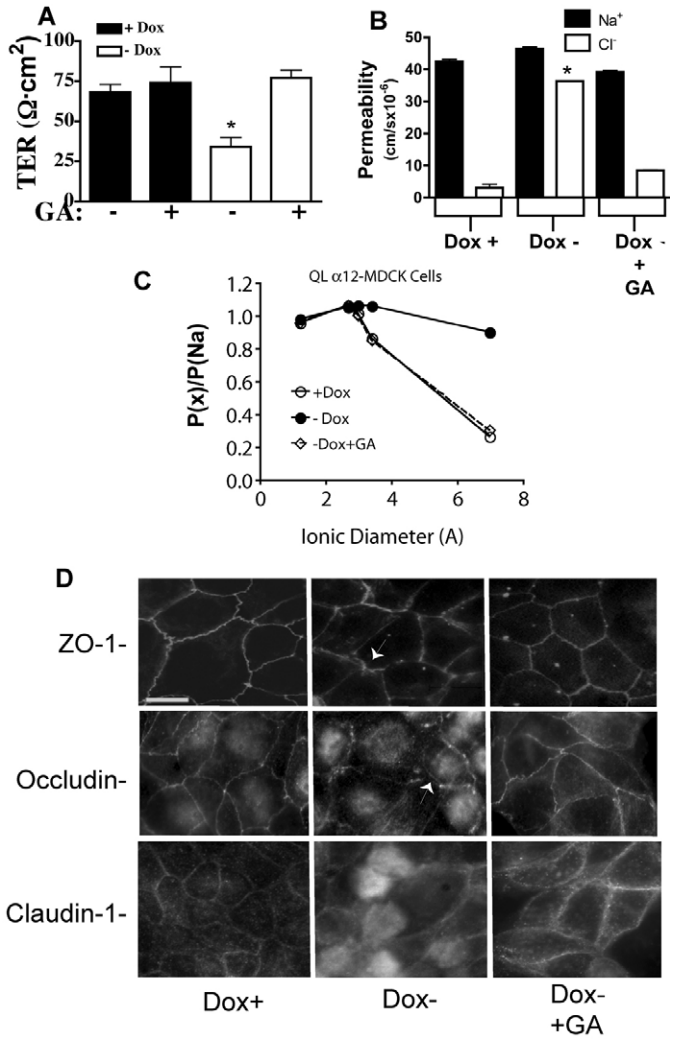

Fig. 4. Hsp90 is necessary for Gα12/Src regulation of permeability and TJ structure. (A) QLα12-MDCK cells in +/–dox and +/–GA (2 μM) for 72 hours were analyzed for TER as described in the Materials and Methods. (B) Sodium and chloride permeability were determined in QLα12-MDCK cells +/–dox and +/–GA as described in Materials and Methods. (C) Effect of GA in QLα12-MDCK cells +/–dox on size selectivity for cation permeability relative to sodium [lithium (Li; 1.2 Å), potassium (K; 2.66 Å), rubidium (Rb; 2.96 Å), cesium (Cs; 3.38 Å) and arginine hydrocholoride (6.96 Å)]. (D) Immunofluorescence microscopy of ZO-1, occludin and claudin 1 in QLα12-MDCK cells +/–dox and –dox +GA. Arrow highlights area of membrane thickening. *P<0.05. Scale bar: 5 μm.

results, inhibiting Src with PP2 prevented the QLα12 resistance to detergent solubilization.

Hsp90 modulates QLα12-mediated increases in paracellular permeability

Gα12 does not directly interact with Src and does not stimulate Src kinase activity (Ma et al., 2000). Hsp90 interacts with both Gα12 (Vaiskunaite et al., 2001; Waheed and Jones, 2002) and Src (Xu and Lindquist, 1993), so we speculated that the Hsp90 chaperone might provide the link between activated Gα12 and Src activation. To test this possibility, we used the Hsp90 inhibitor geldanamycin (GA) (Prodromou et al., 1997). In addition to characterizing the barrier by TER measurement (Fig. 4A), we also measured transepithelial permeability to individual ions using diffusion-potential measurements in Ussing chambers. In un-induced MDCK II cells (+dox), Na^+ permeability was about ninefold higher than Cl^- permeability, indicating the presence of a strong paracellular barrier to anions. Induction of QLα12 expression (–dox) abolished the normal cation selectivity, primarily because of a marked increase in Cl^- permeability (Fig. 4B). In +dox cells, the normal alkali metal selectivity sequence (Li~Na>K>Rb≫Cs) conformed to Eisenman sequence X-XI, suggesting that cation permeation is dependent on electrostatic binding to a strong, negatively charged site within the pore (Diamond and Wright, 1969). Induction of QLα12 almost completely reversed this selectivity (Cs~Rb~K>Na>Li). The resulting sequence (Eisenman I-II) was the same as the order of

free solution mobility of the hydrated ions, suggesting that, under these conditions, cation transport occurred by aqueous diffusion. Finally, induction of QLα12 impaired the size-selective barrier. The normal threefold selectivity of Na^+ (diameter 1.9 Å) over that of arginine, a large organic cation (diameter 7 Å), was completely abolished (Fig. 4C) in QLα12-expressing MDCK cells. Fig. 4 shows TER, sodium and chloride permeability, and size selectivity in QLα12-MDCK cells treated with GA. For all parameters tested, GA had no effect in +dox conditions (Fig. 4). The changes in TER, sodium and chloride permeability, and size selectivity induced with QLα12 expression (–dox) were all reversed with Hsp90 inhibition by GA (Fig. 4A-C). This was identical to the findings with the Src inhibitor PP2 (supplementary material Fig. S2B,C). We next determined whether the morphological changes in the TJ induced by QLα12 expression were reversed by Hsp90 inhibition. Fig. 4D shows ZO-1, occludin and claudin 1 staining of the lateral membrane in control (+dox) QLα12-MDCK cells. With QLα12 expression (–dox), ZO-1 and occludin staining became irregular and diffuse along the plasma membrane, and claudin 1 was predominantly intracellular (Fig. 4D). GA treatment prevented the dislocation of ZO-1, occludin and claudin 1 from the lateral membrane (Fig. 4D, last panel). Finally, inhibition of Hsp90 with GA also prevented the changes in claudin 1 solubility (supplementary material Fig. S3B).

Inhibition of Hsp90 blocks QLα12-stimulated Src activation

Src activity was assessed in QLα12-MDCK cells cultured in +/–dox and +/–GA. Fig. 5A shows the results of western blotting to Src pTyr 419, an indicator of relative Src activity. As previously demonstrated (Meyer et al., 2003), there is a 50% increase in pTyr419 immunoreactivity in –dox QLα12 cells (compared with +dox; Fig. 5A,B). However, inhibiting Hsp90 with GA blocked the QLα12-stimulated increase in Src activity without affecting total Src or occludin levels (Fig. 5A). We expected that GA would inhibit tyrosine phosphorylation of TJ proteins. Because the predominant Gα12-Src target in the TJ is ZO-2 (Fig. 2), we immunoprecipitated ZO-2 from QLα12-MDCK cells +/–dox and +/–GA followed by western blotting for phosphotyrosine (Fig. 5C). Inhibition of Hsp90 blocked Gα12/Src-stimulated phosphorylation of ZO-2. The effects of GA on ZO-1 phosphorylation were inconsistent and it is unclear whether ZO-1 phosphorylation is affected by Hsp90 inhibition (not shown). QLα12 interacts with ZO-1 and can be immunoprecipitated with the ZO-1 complex. To determine whether inhibiting Hsp90 affects this interaction, ZO-1 was immunoprecipitated from QLα12-MDCK cells +/–dox and +/–GA. Fig. 5D shows that, in the absence of QLα12 expression, no QLα12 was detected. Immunoprecipitation of ZO-1 from QLα12-MDCK (–dox) cells co-precipitated a fraction of QLα12. Treatment with GA did not disrupt the QLα12-ZO-1 complex but rather appeared to enhance it; there was a small increase in the amount of co-precipitated QLα12 (n=4, Fig. 5D). The finding suggests that Hsp90 is not required for the Gα12–ZO-1 interaction and is consistent with a model in which Hsp90 is recruited to the complex (discussed later).

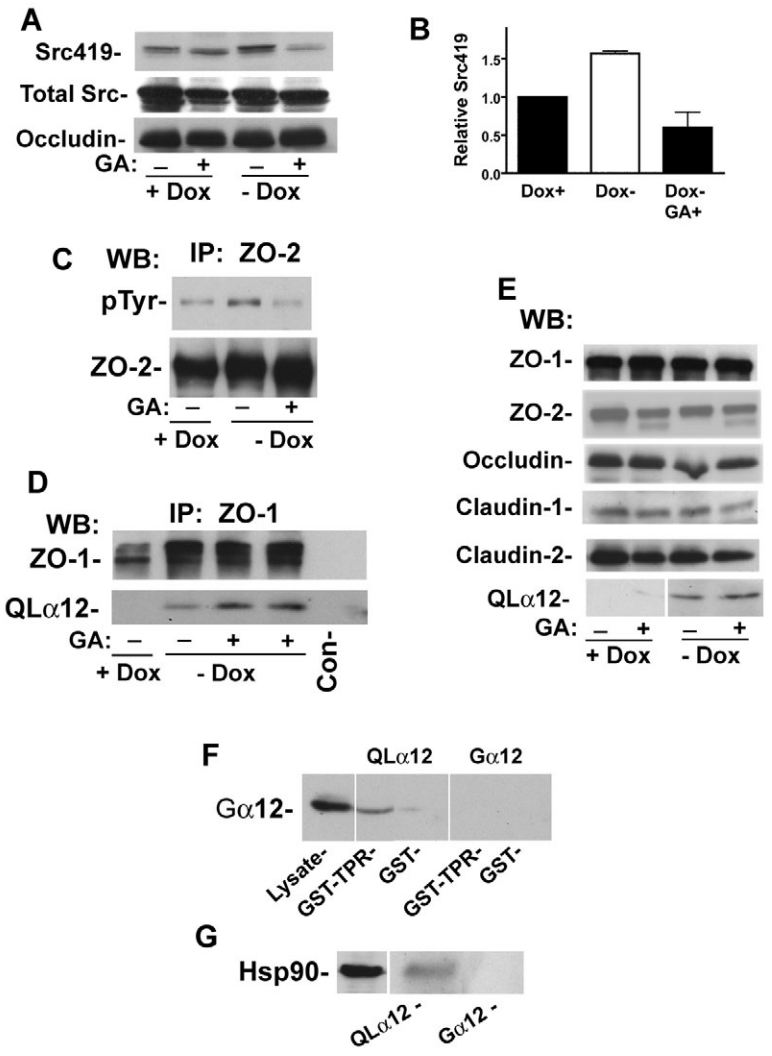

Fig. 5. Hsp90 is a component of the activated Gα12 complex and is necessary for Src activation and ZO-2 phosphorylation. (A) Src activation in QLα12-MDCK cells +/–dox and +/–GA. Identical amounts of cell lysate were analyzed by western blotting with antibodies specific for pTyr-419 as described in the Materials and Methods. Membranes were stripped and reanalyzed for total Src and occludin. (B) Band intensity was quantified as described above and the pTyr-419 immunoreactivity normalized to total Src. The relative amount of pTyr419 for –dox and –dox +GA is shown in comparison to the +dox condition. (C) Phosphotyrosine content of immunoprecipitated ZO-2 from QLα12-MDCK cells +/–dox and +/–GA. ZO-2 was immunoprecipitated and analyzed with 4G10 anti-phosphotyrosine as described above. (D) Interaction of Gα12 with ZO-1 in QLα12-MDCK cells +/–dox and +/–GA. ZO-1 was immunoprecipitated under the specified conditions and precipitates were analyzed for Gα12 by western blotting. Control is lysate with beads alone. (E) Steady-state protein levels of TJ proteins and Gα12 in QLα12-MDCK +/–dox and +/–GA (2 μM). (F) Validation of GST-TPR pull-down of activated Gα12. QLα12- and Gα12-MDCK cells were cultured in –dox, and lysates (~800 μg) were pulled-down with 1 μg GST or GST-TPR, as described in the Materials and Methods, and analyzed by western blotting for Gα12. 10% of the input of wild-type Gα12 is shown in the lysate lane. (G) Hsp90 western blot of GST-TPR pull-downs from Gα12- and QLα12-MDCK cells in –dox.

The steady-state levels of QLα12 and TJ proteins +/–dox and +/–GA in QLα12-MDCK cells were assessed and no significant differences were seen (Fig. 5E). The Hsp90 chaperone complex includes numerous co-chaperones (reviewed in Whitesell and Lindquist, 2005) and a novel N-terminal myristoylated Hsp90 isoform (Hsp90N) is expressed in epithelial cells (Grammatikakis

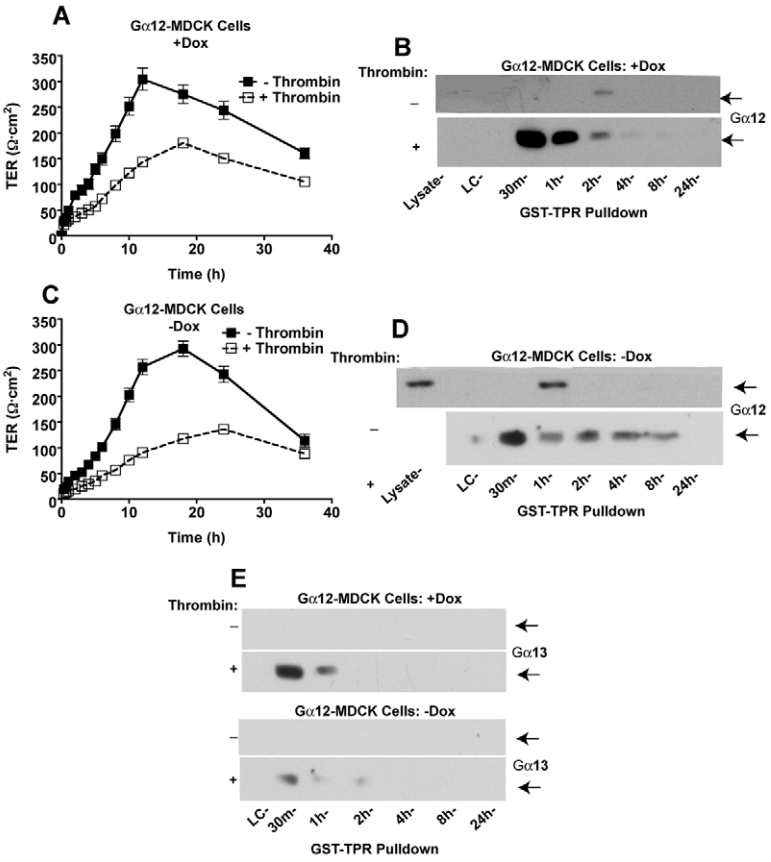

Fig. 6. Endogenous Gα12 is activated during TJ assembly in the calcium switch and thrombin delays TJ assembly. (A) Calcium switch in control Gα12-MDCK cells +dox. Cells were cultured overnight in low calcium (LC; *t*=0) medium and then switched back to normal calcium (NC) medium. TER measurements were obtained at the specified intervals. Thrombin (2 U/ml) was added at *t*=0. Results are the mean ± s.e.m. for *n*=4 at each time point. The experiment was repeated three times with nearly identical results. (B) Western blot of Gα12 +dox cells +/–thrombin analyzed by GST-TPR pull-down at the specified times after the calcium switch. (C) Calcium switch in Gα12-MDCK cells with induced Gα12 expression (–dox). (D) Western blot of Gα12 –dox cells +/–thrombin analyzed by GST-TPR pull-down at the specified times after the calcium switch. The first lane of the top panel shows the induced Gα12 and is ~10% of the protein used for the pull-downs. (E) Western blots for Gα13 on Gα12-MDCK cells +/–dox and +/–thrombin and pulled-down with GST-TPR as described in C. For each panel, the +/–thrombin results were obtained from a single gel.

et al., 2002). However, we were unsuccessful in detecting these proteins in ZO-1 immunoprecipitates under a variety of conditions (not shown). Recently, a GST pull-down assay using GST-TPR [tetratricopeptide domain of protein phosphatase 5 (PP5)] for detecting activated Gα12 has been reported (Yamaguchi et al., 2002; Yamaguchi et al., 2003). This domain selectively interacts with activated Gα12 and Gα13, and has been validated in our Gα12-MDCK cell models (Yanamadala et al., 2007). We reconfirmed the assay using lysates from Gα12- and QLα12-expressing MDCK cells (–dox; Fig. 5F) and studied whether Hsp90 might be a component of the activated Gα12 complex. Fig. 5G shows that Hsp90 is detected in pull-downs of activated (QL) but not wild-type Gα12. This observation is consistent with Hsp90 preferentially interacting with active Gα12. This finding was confirmed and extended with thrombin activation of endogenous Gα12 (discussed later).

A role for Gα12 signaling in regulating TJ assembly

We previously demonstrated that activated Gαi2 and Gαs stimulated TJ assembly in the calcium switch and speculated that there were counter-regulatory Gα-mediated pathways (Saha et al., 1998; Saha et al., 2001). Gα12 was a good candidate to provide the 'brake' on TJ assembly. To address this possibility, we stimulated control MDCK cells (Gα12 in +dox) with thrombin, a known agonist for Gα12/Gα13-coupled pathways. Fig. 6A shows that the addition of thrombin at *t*=0 significantly delays TJ assembly. The GST-TPR pull-down of activated Gα12 (Fig. 6B) revealed that the addition of thrombin leads to robust activation of endogenous Gα12 by 30 minutes and the activation persists through to 2 hours. As expected, endogenous Gα12 was below the detection limit in Gα12-MDCK cells in +dox (lysate lane in Fig. 6B) but, surprising, we detected activation of endogenous Gα12 in non-stimulated cells at 1-2 hours after inducing TJ assembly. We next examined the effects of thrombin on TJ assembly in the calcium switch using Gα12-MDCK cells in –dox. Fig. 6C shows that the effects of thrombin on TJ assembly in Gα12-expressing MDCK cells are similar to the control (+dox; Fig. 6A). Thrombin stimulation resulted in prolonged Gα12 activation (at least 8 hours) in –dox cells (Fig. 6D). Again, there was readily detectable activation of Gα12 without thrombin stimulation seen in GST-TPR pull-downs at approximately 1 hour after the calcium switch. These findings indicate that endogenous Gα12 is activated in non-stimulated MDCK cells undergoing TJ assembly, and that thrombin significantly delays TJ assembly and robustly activates Gα12.

However, thrombin also activates Gα13 and Gαq pathways, and these results do not exclude a role for other G-protein-coupled pathways. The GST-TPR pull-down experiments were probed for Gα13, and Fig. 6E shows that there was no detectable activation of Gα13 in the absence of thrombin stimulation in either +/–dox cells. With thrombin stimulation, there was activation of Gα13 at 30 minutes that was no longer detectable by 1-2 hours after the calcium switch. To determine whether thrombin might regulate TJ assembly through Gα13 or Gαq pathways, the calcium-switch experiments were repeated +/–bradykinin, an agonist reported to activate Gα13, Gαq and other Gα subunits, but not Gα12 (reviewed in Riobo and Manning, 2005). Fig. 7A,B shows that bradykinin stimulation of MDCK cells +/–dox during the calcium switch had no effect on the time-course of TJ assembly. Analysis of GST-TPR pull-downs from bradykinin-stimulated cells confirmed Gα13 activation from 30 minutes to 2 hours with little or no additional activation of Gα12 (Fig. 7C). These results indicate that bradykinin activation of Gα13 and other Gα pathways is unlikely to affect TJ assembly, and are consistent with thrombin regulating TJ assembly through Gα12.

We next investigated whether the inhibition of TJ assembly stimulated by thrombin-Gα12 used Src and Hsp90. The calcium-switch experiments were repeated in control cells (+dox) +/–thrombin and +/–the Src inhibitor PP2 (Fig. 8A) or the Hsp90 inhibitor GA (Fig. 8B). The addition of either inhibitor without thrombin had no effect on the time-course of TER recovery in the calcium switch (Fig. 8A,B). When thrombin was added in the presence of PP2 there was partial recovery in the assembly of the

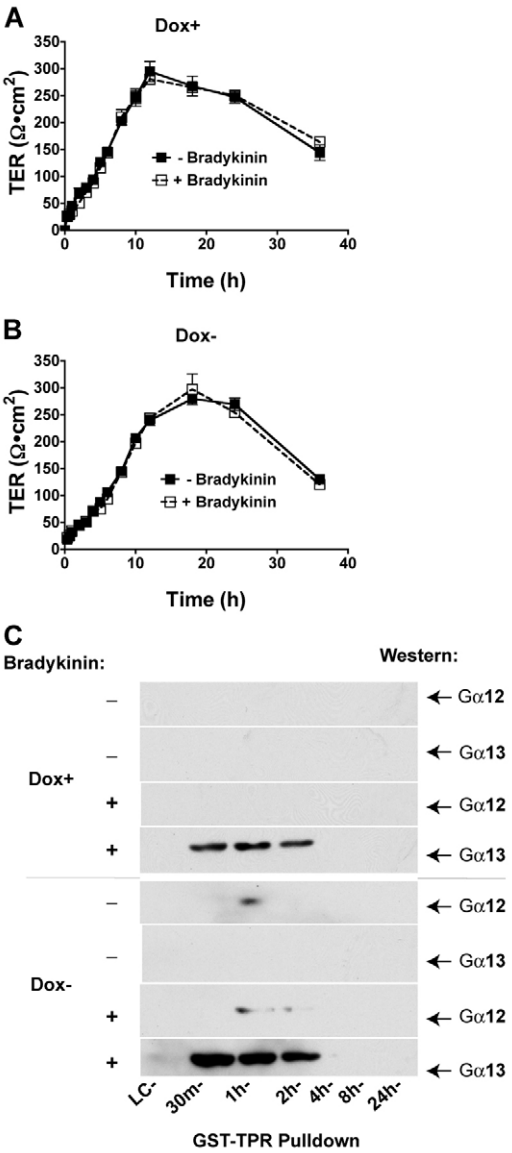

Fig. 7. Bradykinin activates Gα13 without affecting TJ assembly. (A,B) Calcium-switch experiments in Gα12-MDCK cells (A, +dox; B, –dox) +/–bradykinin (100 μM) at *t*=0 as described in Fig. 6. (C) GST-TPR pull-downs from bradykinin-stimulated cells at the specified times after the calcium switch in Gα12-MDCK cells +/–dox. Western blots were probed for Gα12 and were reprobed for Gα13 (designated by arrows). The bradykinin-stimulated cells (+/–dox) were analyzed on a single blot.

barrier (Fig. 8A) and GA completely reversed the thrombin-stimulated delay in barrier assembly (Fig. 8B). These observations suggest that TJ regulation by Gα12 in intact monolayers and during TJ assembly use similar mechanisms.

Finally, we studied whether thrombin is a physiologic regulator of epithelial cell TJs. Fig. 9A shows that the addition of thrombin to a confluent monolayer of control MDCK cells leads to the rapid loss of TER (within minutes). The effects of thrombin were maximal at 1-2 hours and persisted for several more hours before gradually returning to control levels. To determine whether Src and Hsp90 were important to the thrombin signaling, TER values were compared at 40 minutes after the addition of thrombin, bradykinin,

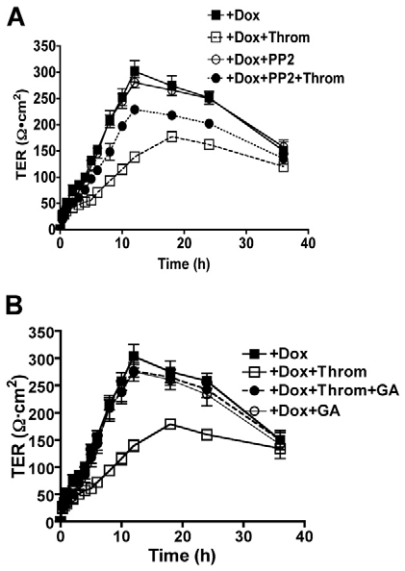

Fig. 8. Inhibiting Src with PP2 and Hsp90 with GA blocks thrombin-stimulated delay in TJ assembly. (A) Calcium switch in +dox Gα12-MDCK cells +/–thrombin and +/–PP2 (10 μM) added at *t*=0. (B) Calcium switch in +dox Gα12-MDCK cells +/–thrombin and +/–GA (2 μM) added at *t*=0.

PP2 and GA (alone and in combination, Fig. 9B). PP2 and GA had no independent effect on TER (Fig. 9B) and, consistent with bradykinin activation of Gα13 but not Gα12, there were no effects of bradykinin on baseline TER (Fig. 9B). Inhibition of Src with PP2 or inhibition of Hsp90 with GA led to normalization of the thrombin-stimulated decrease in TER (Fig. 9B). To confirm the time-course of thrombin stimulation, Gα12 activation and recruitment of Hsp90 to the activated complex are shown in GST-TPR pull-downs at *t*=0, 15 and 30 minutes after the addition of thrombin (Fig. 9C). Neither protein was seen at *t*=0 but, within 15 minutes of thrombin stimulation, both Gα12 and Hsp90 were detected, and at 30 minutes levels of both proteins were increased. Taken together, these findings suggest that thrombin might physiologically regulate TJs via Gα12 activation, recruitment of Hsp90 and Src activation.

Discussion

These studies reveal how Gα12 regulates the TJ in established epithelia and provide the first evidence that Gα12 negatively regulates TJ assembly. It was previously shown that Gα12 interacts with ZO-1, and activated Gα12 disrupts TJ structure and function through Src tyrosine kinases (Meyer et al., 2003; Meyer et al., 2002). Now, it is shown that this mechanism involves disrupting protein-protein interactions within the multi-protein TJ complex. This occurs via Src phosphorylation of ZO-1 and ZO-2, leading to displacement of occludin and claudin 1 from the ZO-1 protein complex. We identified Hsp90 as the intermediate that links activated Gα12 to Src activation. Surprisingly, we identified activation of endogenous Gα12 in the calcium-switch model of TJ biogenesis in the absence of any receptor agonists, suggesting that it might be a crucial checkpoint in TJ assembly. Stimulation of MDCK cells with physiological concentrations of thrombin activates Gα12 but not Gα13, and leads to increased paracellular permeability and delayed TJ assembly through pathways that involve Src and the Hsp90 chaperone complex.

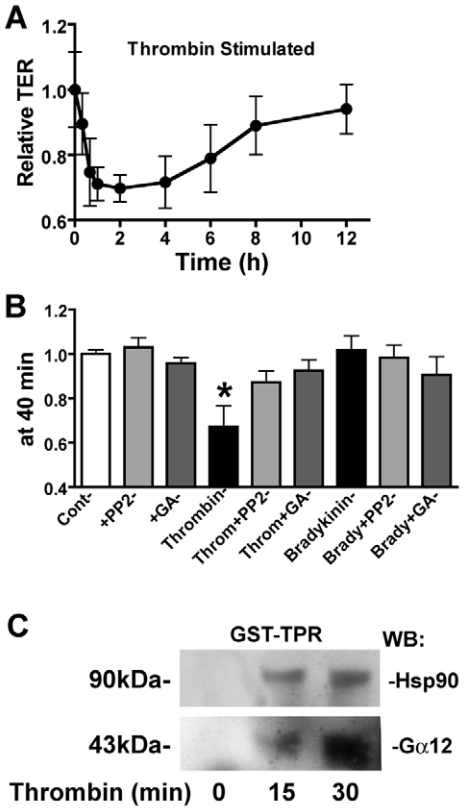

Fig. 9. Thrombin stimulates the loss of barrier function in intact monolayers through Gα12, Src and Hsp90. (A) Confluent monolayers of Gα12-MDCK cells in +dox on Transwell filters were stimulated with thrombin (2 U/ml) at *t*=0 and TER was measured over 12 hours. Results are the mean ± s.e.m. of *n*=4 and were normalized to the untreated control. (B) Monolayers were stimulated at *t*=0 with thrombin (2 U/ml), PP2 (10 μM), GA (0.2 μM), thrombin plus PP2 or GA, bradykinin (100 μM), or bradykinin plus PP2 or GA and compared to vehicle (control). TER was measured at numerous time points. The results (normalized to the untreated control) at 40 minutes are shown (*n*=4 ± s.e.m.). **P*<0.05. (C) Confluent Gα12-MDCK cells in +dox were stimulated at *t*=0 with thrombin and lysates were prepared at *t*=0 (no thrombin), 15 and 30 minutes of stimulation for analysis by GST-TPR pull-down. Western blots to Gα12 and Hsp90 were performed as described above.

Numerous studies have found that tyrosine phosphorylation of TJ proteins perturbs the barrier (Collares-Buzato et al., 1998), and tyrosine kinase phosphorylation of TJ proteins has been shown to be important in the assembly of the junction in models of ATP depletion and reactive oxygen species (Meyer et al., 2001; Tsukamoto and Nigam, 1999). Src mediates oxidative-stress-induced disruption of the TJ in Caco-2 cells (Basuroy et al., 2003) and, in an injury model of mouse proximal tubular cells, Src was localized to the junctions (Sinha et al., 2003). However, there has been little direct evidence of Src within the junctional complex. Our results indicate that a fraction of total Src is found in the TJ complex, and is likely to account for the tyrosine phosphorylation of ZO-1, ZO-2 and possibly other proteins within this membrane microdomain. Nevertheless, the results with genistein and the absence of changes in occludin phosphorylation indicate that additional tyrosine kinases are also important in TJ regulation. The findings in this study are consistent with earlier studies in temperature-sensitive-v-Src-transfected MDCK cells, in which Src phosphorylated ZO-1 and ZO-2 and led to increased permeability (Takeda and Tsukita, 1995). Although ZO-1, ZO-2 and ZO-3 contain an SH3-binding domain, our immunoprecipitation studies could not distinguish direct versus indirect interactions between Src and ZO-1. Although Src could be detected within the ZO-1 complex at baseline, activation of Gα12 led to an increase in the fraction of activated Src interacting with ZO-1 (Fig. 1B). The SH3 domain of ZO-1 is especially important for TJ structure and function; we identified this region of ZO-1 as the interaction site with Gα12 (Meyer et al., 2002) and the SH3 domain alone was shown to rescue delayed TJ assembly in ZO-1-silenced MDCK cells (McNeil et al., 2006). One important role for ZO-1 and related proteins might be to organize and retain a complex of signaling proteins within the TJ in order to provide local regulation in response to changes in the cell environment. The interactions of Gα12 with ZO-1 and the discovery of Src within this complex are consistent with this possibility. We initially identified Gα12 interacting with ZO-1 and ZO-2 (Meyer et al., 2002), and now find that ZO-2 tyrosine phosphorylation was more pronounced than with ZO-1. This finding suggests that, in vivo, the more relevant interaction of Gα12 might be with ZO-2. Future studies will be needed to distinguish between these possibilities.

Our electrophysiological studies suggest that activation of Gα12 induces loss of all aspects of paracellular selectivity. Normally in MDCK cells there is a strong paracellular charge selectivity favoring permeation of cations over anions. Among alkali metal cations, there is selectivity favoring the most heavily hydrated ions (Cereijido et al., 1978; Van Itallie et al., 2001), suggestive of a strong electrostatic cation-binding site in the pore (Diamond and Wright, 1969). Finally, there is normally marked size selectivity favoring permeation of small inorganic cations over bulky organic cations, such as arginine (Yu et al., 2003). We found that QLα12 abolishes all three types of selectivity, suggesting that it induces the opening of large non-selective hydrated pores. This seems unlikely to be due to subtle changes in the expression of specific claudin isoforms and would be more consistent with mechanical disruption of the paracellular barrier by perturbation of the scaffolding of the TJ. Our finding that QLα12 disrupts the interaction between ZO-1 and claudin 1 would be most consistent with this possibility. The implications for the loss of occludin from the ZO-1 complex with Gα12 activation are less clear. Although occludin is an integral membrane protein, it is not required for the formation of an intact TJ (Saitou et al., 1998).

We hypothesized that heat-shock proteins were likely to mediate Gα12-Src signaling. Hsp90 has been widely implicated in stabilizing signaling proteins, including Gα subunits (Busconi et al., 2000) and Src (Xu and Lindquist, 1993; Xu et al., 1999), and Hsp90 directly interacts with Gα12 (but not Gα13) (Vaiskunaite et al., 2001; Waheed and Jones, 2002). Gα12 also activates tyrosine kinases, including Src, but not directly (Jiang et al., 1998; Ma et al., 2000; Nagao et al., 1999). GA treatment of MDCK cells completely inhibited Gα12-stimulated signaling and blocked Src activation (Fig. 5A,B). Inhibition of Hsp90 with GA did not affect the interaction of Gα12 with ZO-1 (Fig. 5D) and we were able to demonstrate Hsp90 in the complex only after Gα12 activation (Fig. 5G and Fig. 9). Other reports support the finding that heat-shock proteins can interact with the TJ; in endothelial cells, an interaction between Hsp70 and ZO-1 has been reported (Lu et al., 2004), and another member of the Hsp70 family, Apg-2, binds to ZO-1, localizes in the TJ and co-precipitates after heat shock (Tsapara et al., 2006). Taken together, we speculate that ZO-1, Src, Gα12 and other components of the TJ complex are in close proximity and/or in

direct contact with each other (see Fig. 10). With activation of Gα12 (QL mutation or thrombin), there is recruitment of Hsp90 to the Gα12–ZO-1 protein complex, facilitating activation of Src (Fig. 10). It is likely that only a small fraction of total cellular Gα12 and Src would be required for signaling in this domain, and it is the association of Gα12 and Src with ZO-1 (or other scaffolding proteins in the junction) that maintains the local organization of the signaling complex.

The mechanisms that epithelia use to assemble a competent TJ involve numerous signaling pathways. The calcium switch is widely used as a model of TJ biogenesis and recapitulates many of the crucial molecular events in epithelial morphogenesis (Balda et al., 1991; Cereijido et al., 1993; Rodriguez-Boulan and Nelson, 1989). The signaling events leading to TJ assembly in the calcium switch use numerous pathways (reviewed in Matter and Balda, 2003). We previously identified roles for several Gα subunits in regulating the assembly of the TJ in the calcium switch (Denker et al., 1996; Saha et al., 1998; Saha et al., 2001) but in each case the kinetics of TJ formation were accelerated. We hypothesized that other Gα subunits were likely to counter-regulate this process and now identify Gα12 as a crucial check-point negatively regulating TJ assembly. The mechanism(s) leading to activation of Gα12 during this process are currently being investigated and could involve activation of calcium-sensing receptors (CaR) that couple to Gα12 in MDCK cells (Huang et al., 2004). Thrombin robustly activates Gα12, significantly delays TJ assembly and affects baseline properties within minutes. The physiological importance of thrombin regulation of epithelial cell permeability is supported by studies of intestinal PAR2 receptors; in these studies, thrombin led to increased permeability and redistribution of ZO-1 and occludin from the TJ (Jacob et al., 2005). Other Gα12/Gα13 receptor agonists such as LPA also affect barrier function (Postma et al., 1998; Schulze et al., 1997).

Taken together, these results suggest that there is a balance between signaling pathways favoring either TJ assembly or disassembly. Gα12/Src signaling is likely to be a pivotal mechanism in the pathways leading to increased permeability and TJ disassembly (Fig. 10). This possibility is supported by the observation that similar signaling mechanisms, via Gα12, Hsp90 and Src, are important for regulating paracellular permeability in established monolayers and for slowing TJ assembly. We propose that Gα12 activation is important in the normal regulation of TJ function and in pathophysiological conditions that disrupt TJs (such as ischemic renal injury). Insights from our studies suggest that inhibiting Gα12 and Src might permit more rapid recovery of epithelial cell function after injury.

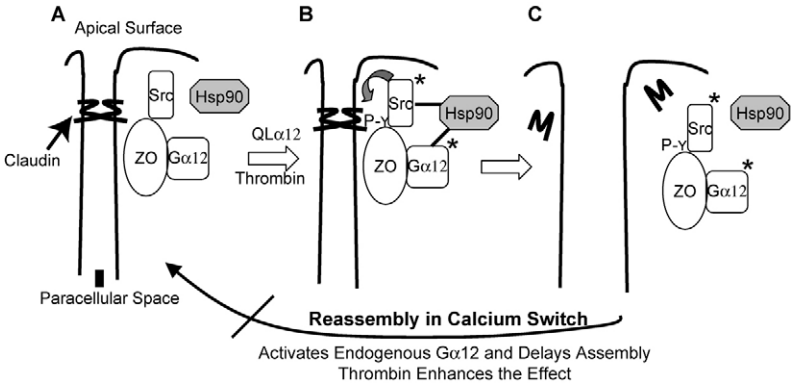

Fig. 10. Gα12 as a check-point in TJ regulation. At baseline (A), claudins from neighboring cells interact with each other in the paracellular space and with ZO-1 in the TJ. The TJ protein complex contains numerous proteins. In this figure, ZO-1, ZO-2 and ZO-3 are designated ZO. Src might interact directly or indirectly with the ZO complex. Gα12 directly interacts with ZO-1 and ZO-2, and Hsp90 is probably not constitutively localized in this domain but is recruited to the activated Gα12 complex (denoted with * in B). Activated Gα12 (QL mutation or thrombin) activates Src (denoted with * in B) leading to increased tyrosine phosphorylation of ZO-1 and ZO-2 (P-Y). (C) Phosphorylation of ZO-1 and ZO-2 leads to disruption of the ZO-1 protein complex, intracellular localization of claudin 1 and loss of barrier function. In addition to the loss of barrier function, under some conditions of persistent activation, this could lead to persistent disassembly of the TJ. Once TJs are disrupted and stimulated to reassemble (as in the calcium switch), activation of Gα12 (using Hsp90 and Src) leads to a brake on TJ assembly.

Materials and Methods

Reagents

GST-TPR was provided by Manabu Negishi (University of Tokyo, Japan). Rabbit polyclonal anti-Gα12 and c-Src were from Santa Cruz Biotechnology (Santa Cruz, CA); anti-ZO-1 rat monoclonal antibody (R40.76) was provided by D. Goodenough (Harvard University, MA); rabbit anti-ZO-1, ZO-2, occludin, claudin 1 and claudin 2 were from Zymed Laboratories (San Francisco, CA); anti-pTyr^{419}- and anti-pTyr^{520}-Src were from Biosource International (Camarillo, CA); monoclonal anti-phosphotyrosine 4G10 was from Upstate Biotechnology (Lake Placid, NY); and rabbit Hsp-90 (SPA-846) and mouse Hsp70 (SPA-820) were from Stressgen (Victoria, BC). The Hsp90N, Cdc37 antibodies have been previously described (Grammatikakis et al., 2002). The inhibitors PP2 and genistein were from Calbiochem (San Diego, CA), and bradykinin and GA were from Sigma (St Louis, MO).

Cell culture

Establishment, characterization and culture conditions for Tet-Off MDCK II cell lines (Clontech, Mountain View, CA) with inducible wild-type Gα12 and QLα12 expression were previously described (Meyer et al., 2002). Briefly, cells were maintained in Dulbecco's modified Eagle's medium (Cellgro, Herndon, VA) containing 5% Tet system-approved FBS (Clontech, Mountain View, CA), 100 μg/ml G418 (Cellgro), 50 IU/ml penicillin, and 50 μg/ml streptomycin (Gibco, Carlsbad, CA), 100 μg/ml hygromycin (Roche, Indianapolis, IN) and 40 ng/ml doxycycline (Sigma, St Louis, MO).

Transepithelial resistance

MDCK cells were plated at confluency on polycarbonate Transwell filters (Transwell, Costar) at ~4×10^5 cells/cm^2 and maintained in culture medium +dox for 72 hours. Monolayers were maintained in +dox medium or switched to –dox for 72 hours in the presence and absence of inhibitors, and TER was measured using the Millicell Electrical Resistance system (Millipore, Bedford, MA) as previously described (Denker et al., 1996). Measurements (in Ω/cm^2) are expressed as a mean of the original readings (n=3 to 5) after subtraction of background values.

Diffusion potential measurements

Measurements were performed as described previously (Yu et al., 2003). In brief, cells cultured on Snapwell filters (Corning) were mounted in Ussing chambers that were filled with Ringer solution (150 mM NaCl, 2 mM $CaCl_2$, 1 mM $MgCl_2$, 10 mM glucose, 10 mM HEPES, pH 7.4) at 37°C. To determine the NaCl dilution potential, the solution in the basolateral chamber was replaced by a modified Ringer solution containing 75 mM NaCl (osmolarity adjusted with mannitol) and the voltage was read immediately under open-circuit conditions. The basolateral solution was then sequentially replaced by Ringer solution in which NaCl was substituted by 150 mM LiCl, KCl, RbCl, CsCl and arginine chloride, to measure the bi-ionic potential. Relative permeability ratios were calculated from these diffusion-potential data using the Goldman-Hodgkin-Katz equation. The absolute permeabilities to Na^+ and Cl^- were derived by the method of Kimizuka and Koketsu (Kimizuka and Koketsu, 1964).

Immunoprecipitation and western blotting

Gα12- or QLα12-expressing MDCK cells were cultured +/–dox. Monolayers were scraped in lysis buffer [100 mM NaCl, 2 mM EDTA, 10 mM HEPES, pH 7.5, 1 mM $NaVO_4$, 25 mM NaF, 1 mM phenylmethylsulfonylfluoride (PMSF), 1% Triton X-100, 0.5% sodium deoxycholate, 0.1% SDS, 1 mM PMSF and proteases inhibitors (Roche, Indianapolis, IN)], frozen/thawed, triturated and centrifuged. Immunoprecipitations of ZO-1 (with R40.76), ZO-2, occludin, claudin 1 and claudin

2 were done with protein-A–sepharose or goat affinity-purified rat IgG beads (MP Biomedicals, Aurora, OH) overnight at 4°C. Beads were centrifuged, washed three times and proteins eluted in SDS-PAGE sample buffer. SDS-PAGE was followed by western blot transfer as previously described (Meyer et al., 2003). After blocking and washing, primary antibodies to ZO-1 (rat 1:10 or rabbit 1:100), ZO-2 (1:1000), occludin (1:1000), claudin 1 (1:750) and claudin 2 (1:750) were added overnight followed by incubation with secondary horseradish-peroxidase-conjugated antibodies for 1 hour. Signal was detected with SuperSignal West Pico horseradish peroxidase substrate system (Pierce) and autoradiography (Biomax MR, Eastman Kodak, Rochester, NY).

Detergent extractions

Detergent-soluble and -insoluble fractions were prepared as described previously (Singh and Harris, 2004). Extractions were done at 72 hours after switching to –dox using extraction buffer (10 mM HEPES, pH 7.2, 1% triton X-100, 100 mM NaCl and protease inhibitors). Cells were scraped, incubated for 20 minutes at 4°C and centrifuged. The supernatant (S; soluble fraction) was collected and the pellet resuspended in solubilization buffer (10 mM HEPES, pH 7.2, 1% SDS, 100 mM NaCl and protease inhibitors). The cell suspension was sonicated, incubated for 20 minutes at 4°C and centrifuged for 20 minutes. The resulting supernatant was labeled I (insoluble fraction). Equivalent volumes of each fraction were analyzed by SDS-PAGE and western blotting.

Phosphotyrosine immunoblots

The Gα12- or QLα12-expressing MDCK cells +/–dox were scraped with 20 mM HEPES, pH 7.0, 1% Triton X-100, 2 mM EGTA, 3.5 mM EDTA, 30 mM NaF, 40 mM β-glycerophosphate, pH 7.2, 20 mM sodium pyrophosphate, 1 mM sodium orthovanadate, 1 mM PMSF and protease inhibitors. Immunoprecipitations, SDS-PAGE and western blotting were performed as described above, except that nitrocellulose was blocked with 3% non-fat dry milk for 60 minutes at room temperature. Primary-antibody incubation with anti-phosphotyrosine, 4G10 (1:1000) was done overnight at 4°C and then processed as described above.

Immunohistochemistry and confocal imaging

Gα12- and QLα12 MDCK cells were plated on Transwell filters and maintained +/–dox for 72 hours. The cells were fixed with 4% paraformaldehyde (EM Sciences, Fort Washington, PA) in PBS for 10 minutes at room temperature and rinsed with PBS three times for 5 minutes. The cells were blocked for 45 minutes at room temperature in PBS-Triton X 0.02% and 5% (w/v) BSA (PBS-T). Primary antibodies were diluted 1:200 in PBS-T and incubated at room temperature for 1.5 hours. Texas red or fluorescein-isothiocyanate-conjugated secondary antibodies (Pierce, Rockford, IL) were diluted 1:100 in 0.05% Triton X-100 in PBS. Filters were washed three times with PBS for 5 minutes, mounted, and imaging was carried out using a Nikon TE 2000E2 microscope, captured to a COOLSNAP HQ cooled CCD (Photometrics; Tuscon, AZ) and IPLab software (Scanalytics; Fairfax, VA). Confocal imaging was carried out using a CSU21 UltraView Spinning Disk Confocal Imager (Perkin Elmer; Boston, MA) and three-dimensional reconstruction performed in the Volocity software package (Improvision; Lexington, MA). Cells were imaged from the apical region to within a few microns of the basolateral surface to reduce autofluorescence originating from the basolateral membrane filter. Specific images were assembled using Photoshop software (Adobe; San Jose, CA) and incorporated into figures using Illustrator (Adobe; San Jose, CA).

Calcium-switch assay

Gα12-MDCK cells (+/–dox) were plated at confluency on Transwells and allowed to equilibrate for 48-72 hours. Monolayers were rinsed three times and incubated in low calcium (LC) medium (SMEM; Invitrogen) +/–dox, containing 5% dialyzed FBS for 18 hours. At *t*=0, the medium was changed to normal calcium (NC) medium +/–dox and TER values obtained at specific times. Agonists (thrombin 2U/ml and bradykinin 100 μM) and inhibitors (PP2, 10 μM and GA 0.2 μM) were added at *t*=0.

GST-TPR pull-down

GST-TPR was purified from bacterial lysates as described (Meyer et al., 2002). MDCK cells were cultured under specified conditions and cell lysates prepared in lysis buffer (50 mM HEPES, pH 7.5, 1 mM EDTA, 3 mM DTT, 10 mM $MgSO_4$, 1.0% polyoxyethylene-10-lauryl ether and protease inhibitors). 1 μg of GST-TPR or GST alone were coupled to glutathione-agarose beads (Amersham Pharmacia), added to 800 μg of total protein and rocked overnight at 4°C. Samples were centrifuged, the beads were washed three times with PBS+0.1% Triton X-100 and resuspended in lysis buffer containing SDS-PAGE sample buffer. Eluted samples were analyzed by SDS-PAGE and western blotting.

Quantification and statistics

Western blots were scanned using an Epson 1640 desktop scanner and band intensity quantified using NIH Image (Wayne Rasband) after subtracting background and determining linear range. Statistics were done in GraphPad Prism (San Diego, CA). Significance was determined by using two-tailed *t*-test.

This work was supported by grants from the National Institutes of Health (GM55223 and DK65932 to B.M.D.; DK062283 to A.S.L.Y.) and the American Heart Association Fellowship (0325684T to E.S.).

References

Balda, M. S., Gonzalez-Mariscal, L., Macias-Silva, M., Torres-Marquez, M. E., Garcia Sainz, J. A. and Cereijido, M. (1991). Assembly and sealing of tight junctions: possible participaton of G-proteins, phospholipase C, protein kinase C and calmodulin. *J. Membr. Biol.* **122**, 193-202.

Basuroy, S., Sheth, P., Kuppuswamy, D., Balasubramanian, S., Ray, R. M. and Rao, R. K. (2003). Expression of kinase-inactive c-Src delays oxidative stress-induced disassembly and accelerates calcium-mediated reassembly of tight junctions in the Caco-2 cell monolayer. *J. Biol. Chem.* **278**, 11916-11924.

Blumer, J. B., Chandler, L. J. and Lanier, S. M. (2002). Expression analysis and subcellular distribution of the two G-protein regulators AGS3 and LGN indicate distinct functionality. Localization of LGN to the midbody during cytokinesis. *J. Biol. Chem.* **277**, 15897-15903.

Busconi, L., Guan, J. and Denker, B. M. (2000). Degradation of heterotrimeric Gαo subunits via the proteosome pathway is induced by the hsp90-specific compound geldanamycin. *J. Biol. Chem.* **275**, 1565-1569.

Cereijido, M., Robbins, E. S., Dolan, W. J., Rotunno, C. A. and Sabatini, D. D. (1978). Polarized monolayers formed by epithelial cells on a permeable and translucent support. *J. Cell Biol.* **77**, 853-880.

Cereijido, M., Gonzalez-Mariscal, L., Conreras, R. G., Gallardo, J. M., Garcia-Villegas, R. and Valdes, J. (1993). The making of a tight junction. *J. Cell Sci. Suppl.* **17**, 127-132.

Collares-Buzato, C. B., Jepson, M. A., Simmons, N. L. and Hirst, B. H. (1998). Increased tyrosine phosphorylation causes redistribution of adherens junction and tight junction proteins and perturbs paracellular barrier function in MDCK epithelia. *Eur. J. Cell Biol.* **76**, 85-92.

de Almeida, J. B., Holtzman, E. J., Peters, P., Ercolani, L., Ausiello, D. A. and Stow, J. L. (1994). Targeting of chimeric Gαi proteins to specific membrane domains. *J. Cell Sci.* **107**, 507-515.

Denker, B. M. and Nigam, S. K. (1998). Molecular structure and assembly of the tight junction. *Am. J. Physiol.* **274**, F1-F9.

Denker, B. M., Saha, C., Khawaja, S. and Nigam, S. K. (1996). Involvement of a heterotrimeric G protein α subunit in tight junction biogenesis. *J. Biol. Chem.* **271**, 25750-25753.

Diamond, J. M. and Wright, E. M. (1969). Biological membranes: The physical basis of ion and nonelectrolyte selectivity. *Annu. Rev. Physiol.* **31**, 581-646.

Dodane, V. and Kachar, B. (1996). Identification of isoforms of G proteins and PKC that colocalize with tight junctions. *J. Membr. Biol.* **149**, 199-209.

D'Souza, T., Agarwal, R. and Morin, P. J. (2005). Phosphorylation of claudin-3 at threonine 192 by cAMP-dependent protein kinase regulates tight junction barrier function in ovarian cancer cells. *J. Biol. Chem.* **280**, 26233-26240.

Ercolani, L., Stow, J. L., Boyle, J. F., Holtzman, E. J., Lin, H., Grove, J. R. and Ausiello, D. A. (1990). Membrane localization of the pertussis toxin-sensitive G-protein subunits αi2 and αi3 and expression of a metallothionein- αi2 fusion gene in LLC-PK1 cells. *Proc. Natl. Acad. Sci. USA* **87**, 4635-4639 [published erratum appears in *Proc. Natl. Acad. Sci. USA* 87, 7344].

Furuse, M., Fujita, K., Hiiragi, T., Fujimoto, K. and Tsukita, S. (1998). Claudin-1 and -2: novel integral membrane proteins localizing at tight junctions with no sequence similarity to occludin. *J. Cell Biol.* **141**, 1539-1550.

Grammatikakis, N., Vultur, A., Ramana, C. V., Siganou, A., Schweinfest, C. W., Watson, D. K. and Raptis, L. (2002). The role of Hsp90N, a new member of the Hsp90 family, in signal transduction and neoplastic transformation. *J. Biol. Chem.* **277**, 8312-8320.

Hamilton, S. E. and Nathanson, N. M. (1997). Differential localization of G proteins, Gαo and Gαi1, -2, and -3 in polarized epithelial MDCK cells. *Biochem. Biophys. Res. Commun.* **234**, 1-7.

Huang, C., Hujer, K. M., Wu, Z. and Miller, R. T. (2004). The Ca^{2+}-sensing receptor couples to Gα12/13 to activate phospholipase D in Madin-Darby canine kidney cells. *Am. J. Physiol. Cell Physiol.* **286**, C22-C30.

Jacob, C., Yang, P. C., Darmoul, D., Amadesi, S., Saito, T., Cottrell, G. S., Coelho, A. M., Singh, P., Grady, E. F., Perdue, M. et al. (2005). Mast cell tryptase controls paracellular permeability of the intestine. Role of protease-activated receptor 2 and β-arrestins. *J. Biol. Chem.* **280**, 31936-31948.

Jiang, Y., Ma, W., Wan, Y., Kozasa, T., Hattori, S. and Huang, X. Y. (1998). The G protein Gα12 stimulates Bruton's tyrosine kinase and a rasGAP through a conserved PH/BM domain. *Nature* **395**, 808-813.

Kimizuka, H. and Koketsu, K. (1964). Ion transport through cell membrane. *J. Theor. Biol.* **6**, 290-305.

Lee, D. B., Huang, E. and Ward, H. J. (2006). Tight junction biology and kidney dysfunction. *Am. J. Physiol. Renal Physiol.* **290**, F20-F34.

Lu, T. S., Chen, H. W., Huang, M. H., Wang, S. J. and Yang, R. C. (2004). Heat shock treatment protects osmotic stress-induced dysfunction of the blood-brain barrier through preservation of tight junction proteins. *Cell Stress Chaperones* **9**, 369-377.

Ma, Y. C., Huang, J., Ali, S., Lowry, W. and Huang, X. Y. (2000). Src tyrosine kinase is a novel direct effector of G proteins. *Cell* **102**, 635-646.

Matter, K. and Balda, M. S. (2003). Signalling to and from tight junctions. *Nat. Rev. Mol. Cell Biol.* **4**, 225-236.

McNeil, E., Capaldo, C. T. and Macara, I. G. (2006). Zonula occludens-1 function in the assembly of tight junctions in Madin-Darby canine kidney epithelial cells. *Mol. Biol. Cell* **17**, 1922-1932.

Meyer, T. N., Schwesinger, C., Ye, J., Denker, B. M. and Nigam, S. K. (2001). Reassembly of the tight junction after oxidative stress depends on tyrosine kinase activity. *J. Biol. Chem.* **276**, 22048-22055.

Meyer, T. N., Schwesinger, C. and Denker, B. M. (2002). Zonula occludens-1 is a scaffolding protein for signaling molecules. Gα12 directly binds to the Src homology 3 domain and regulates paracellular permeability in epithelial cells. *J. Biol. Chem.* **277**, 24855-24858.

Meyer, T. N., Hunt, J., Schwesinger, C. and Denker, B. M. (2003). Gα12 regulates epithelial cell junctions through Src tyrosine kinases. *Am. J. Physiol. Cell Physiol.* **285**, C1281-C1293.

Nagao, M., Kaziro, Y. and Itoh, H. (1999). The Src family tyrosine kinase is involved in Rho-dependent activation of c-Jun N-terminal kinase by Gα12. *Oncogene* **18**, 4425-4434.

Neer, E. J. (1995). Heterotrimeric G proteins: organizers of transmembrane signals. *Cell* **80**, 249-257.

Nusrat, A., Turner, J. R. and Madara, J. L. (2000). Molecular physiology and pathophysiology of tight junctions. IV. Regulation of tight junctions by extracellular stimuli: nutrients, cytokines, and immune cells. *Am. J. Physiol. Gastrointest. Liver Physiol.* **279**, G851-G857.

Pimplikar, S. W. and Simons, K. (1993). Role of heterotrimeric G proteins in polarized membrane transport. *J. Cell Sci. Suppl.* **17**, 27-32.

Postma, F. R., Hengeveld, T., Alblas, J., Giepmans, B. N., Zondag, G. C., Jalink, K. and Moolenaar, W. H. (1998). Acute loss of cell-cell communication caused by G protein-coupled receptors: a critical role for c-Src. *J. Cell Biol.* **140**, 1199-1209.

Prodromou, C., Roe, S. M., O'Brien, R., Ladbury, J. E., Piper, P. W. and Pearl, L. H. (1997). Identification and structural characterization of the ATP/ADP-binding site in the Hsp90 molecular chaperone. *Cell* **90**, 65-75.

Riobo, N. A. and Manning, D. R. (2005). Receptors coupled to heterotrimeric G proteins of the G12 family. *Trends Pharmacol. Sci.* **26**, 146-154.

Rodriguez-Boulan, E. and Nelson, W. J. (1989). Morphogenesis of the polarized epithelial cell phenotype. *Science* **245**, 718-725.

Saha, C., Nigam, S. K. and Denker, B. M. (1998). Involvement of Gαi2 in the maintenance and biogenesis of epithelial cell tight junctions. *J. Biol. Chem.* **273**, 21629-21633.

Saha, C., Nigam, S. K. and Denker, B. M. (2001). Expanding role of G proteins in tight junction regulation: Gα(s) stimulates TJ assembly. *Biochem. Biophys. Res. Commun.* **285**, 250-256.

Saitou, M., Fujimoto, K., Doi, Y., Itoh, M., Fujimoto, T., Furuse, M., Takano, H., Noda, T. and Tsukita, S. (1998). Occludin-deficient embryonic stem cells can differentiate into polarized epithelial cells bearing tight junctions. *J. Cell Biol.* **141**, 397-408.

Schulze, C., Smales, C., Rubin, L. L. and Staddon, J. M. (1997). Lysophosphatidic acid increases tight junction permeability in cultured brain endothelial cells. *J. Neurochem.* **68**, 991-1000.

Singh, A. B. and Harris, R. C. (2004). Epidermal growth factor receptor activation differentially regulates claudin expression and enhances transepithelial resistance in Madin-Darby canine kidney cells. *J. Biol. Chem.* **279**, 3543-3552.

Sinha, D., Wang, Z., Price, V. R., Schwartz, J. H. and Lieberthal, W. (2003). Chemical anoxia of tubular cells induces activation of c-Src and its translocation to the zonula adherens. *Am. J. Physiol. Renal Physiol.* **284**, F488-F497.

Stow, J. L., de Almeida, J. B., Narula, N., Holtzman, E. J., Ercolani, L. and Ausiello, D. A. (1991). A heterotrimeric G protein, Gαi3, on Golgi membranes regulates the secretion of a heparan sulfate proteoglycan in LLC-PK1 epithelial cells. *J. Cell Biol.* **114**, 1113-1124.

Takeda, H. and Tsukita, S. (1995). Effects of tyrosine phosphorylation on tight junctions in temperature-sensitive v-src-transfected MDCK cells. *Cell Struct. Funct.* **20**, 387-393.

Tsapara, A., Matter, K. and Balda, M. S. (2006). The heat shock protein Apg-2 binds to the tight junction protein ZO-1 and regulates transcriptional activity of ZONAB. *Mol. Biol. Cell* **17**, 1322-1330.

Tsukamoto, T. and Nigam, S. K. (1999). Role of tyrosine phosphorylation in the reassembly of occludin and other tight junction proteins. *Am. J. Physiol.* **276**, F737-F750.

Tsukita, S., Furuse, M. and Itoh, M. (2001). Multifunctional strands in tight junctions. *Nat. Rev. Mol. Cell Biol.* **2**, 285-293.

Vaiskunaite, R., Kozasa, T. and Voyno-Yasenetskaya, T. A. (2001). Interaction between the Gα subunit of heterotrimeric G(12) protein and Hsp90 is required for Gα12 signaling. *J. Biol. Chem.* **276**, 46088-46093.

Van Itallie, C., Rahner, C. and Anderson, J. M. (2001). Regulated expression of claudin-4 decreases paracellular conductance through a selective decrease in sodium permeability. *J. Clin. Invest.* **107**, 1319-1327.

Waheed, A. A. and Jones, T. L. (2002). Hsp90 interactions and acylation target the G protein Gα12 but not Gα13 to lipid rafts. *J. Biol. Chem.* **277**, 32409-32412.

Whitesell, L. and Lindquist, S. L. (2005). HSP90 and the chaperoning of cancer. *Nat. Rev. Cancer* **5**, 761-772.

Xu, Y. and Lindquist, S. (1993). Heat-shock protein hsp90 governs the activity of pp60v-src kinase. *Proc. Natl. Acad. Sci. USA* **90**, 7074-7078.

Xu, Y., Singer, M. A. and Lindquist, S. (1999). Maturation of the tyrosine kinase c-src as a kinase and as a substrate depends on the molecular chaperone Hsp90. *Proc. Natl. Acad. Sci. USA* **96**, 109-114.

Yamaguchi, Y., Katoh, H., Mori, K. and Negishi, M. (2002). Gα12 and Gα13 interact with Ser/Thr protein phosphatase type 5 and stimulate its phosphatase activity. *Curr. Biol.* **12**, 1353-1358.

Yamaguchi, Y., Katoh, H. and Negishi, M. (2003). N-terminal short sequences of α subunits of the G12 family determine selective coupling to receptors. *J. Biol. Chem.* **278**, 14936-14939.

Yanamadala, V., Negoro, H., Gunaratnam, L., Kong, T. and Denker, B. M. (2007). Gα12 stimulates apoptosis in epithelial cells through JNK1-mediated Bcl-2 degradation and up-regulation of IκBα. *J. Biol. Chem.* **282**, 24352-24363.

Yu, A. S., Enck, A. H., Lencer, W. I. and Schneeberger, E. E. (2003). Claudin-8 expression in Madin-Darby canine kidney cells augments the paracellular barrier to cation permeation. *J. Biol. Chem.* **278**, 17350-17359.